Waveform Modelling of 2009 Bhutan Earthquake of Magnitude 6.1 (Mw) Using Local Network Data of North East India

Santanu Baruah and Midusmita Boruah

Keywords Bhutan earthquake · Waveform inversion · Transverse tectonics

1 Introduction

A strong earthquake of Mw 6.1 struck Bhutan on September 21, 2009 with casualties of several people. The epicentre of the event was given at latitude 27.34° N and longitude 91.41° E, and depth ~ 10 km (USGS report; http://earthquake.usgs.gov). Shaking from the earthquake was felt in the Bhutan, Tibet and in the adjoining North East region of India including Bangladesh.

The objective of this work is to carry out the numerical modeling of the 21st September 2009 Bhutan earthquake and its aftershocks and the identification of physical mechanism based on 1D velocity model. To accomplish this, modeling of main shock and its aftershocks is carried out through waveform inversion which in turn help in understanding the physics of the earthquake process by characterizing the associated fault. The reason for using the waveform inversion tool is that it enables estimation of reliable focal mechanism solutions that estimates seismic moment and moment magnitude, quantifying the earthquake to the extent. Fault-plane solution thus obtained are tried to correlate with the local geology in order to identify the causative fault of the Bhutan Himalaya 2009 earthquake. Additionally, to identify the true fault plane orientation, the H (Hypocentre)—C (Centroid) method (Zahradnik et al. 2008) was used with combined knowledge of the centroid position, MT solution (nodal planes) and hypocentre parameter.

S. Baruah (✉)
Geosciences & Technology Division, CSIR-North East Institute of Science and Technology, Jorhat 785006, Assam, India
e-mail: santanub27@gmail.com

M. Boruah
Department of Applied Geology, Dibrugarh University, Dibrugarh 786004, Assam, India

S. D'Amico (ed.), *Moment Tensor Solutions*, Springer Natural Hazards,
https://doi.org/10.1007/978-3-319-77359-9_18

2 Tectonic Settings of Bhutan Himalaya

The Himalaya is the largest orogenic belt of the world form by the collision between Indian subcontinent and Tibet about 50 Ma ago (Gansser 1964; McKenzie and Sclater 1971; Molnar and Tapponnier 1975; Mitchell 1981; Curry et al. 1982; Zhao et al. 1993; Nandy 2001). Main Boundary Thrust (MBT) and the Main Central Thrust (MCT) are the major tectonic features that are traversing Bhutan Himalaya to the north, albeit a circular overturned of the later (Ravi Kumar et al. 2012; Pradhan et al. 2013). The MCT in Bhutan Himalaya has taken a curvilinear loop shape indicating thicker sediments (Fig. 1). Based on the known geology, geophysics and teleseismic hypocentral data Seeber and Armbruster (1981) first proposed a conceptual tectonic model of the Himalaya known as Steady-state model. The model consists of the underthrusted Indian plate beneath the Himalaya (known as plane of detachment), overriding Tethyan slab and the Himalayan sedimentary wedge, which is decoupled from the two converging slabs. In this model, the MBT and the MCT are two active thrusts and are contemporaneous features. Further north, below the MCT lies the *ramp,* named *basement thrust front* that accumulates the tectonic stress due to northward movement of the Indian plate, and abrupt release is believed to be the main cause of earthquakes on the plane of detachment at a shallower depth (0–20 km).

The Bhutan Himalaya is different from the western section of the Himalayas with the presence of the Kakhtang thrust (KT) which is an out of sequence thrust located between the MCT and the STDS (South Tibetan Detachment System) (Gansser 1993; Grujic et al. 1996, 2002, 2006; Drukpa et al. 2006). Seismic pattern in relationship to the major tectonic faults and lineaments of the region have been examined by several researchers in the past (e.g. Seeber and Armbruster 1981; Ni and Barazangi 1984; Fitch 1970; Baranowski et al. 1984; Searle 1996; Chen and Kao 1996). It is found that most of the earthquakes in this region lie between the MCT and the MBT in the 50 km wide relatively narrow belt and are mostly concentrated south of the MCT (Ni and Barazangi 1984). The fault plane solutions of the past studies as well as from Harvard G-CMT, indicate that most of the earthquakes along the Himalayan region are thrust faulting (Fitch 1970; Baranowski et al. 1984; Searle 1996; Chen and Kao 1996). The slip vectors of these solutions are found to be perpendicular to the mountain ranges with steeper plunges (~25°) in the western Himalaya, in contrast to shallow plunges of (~10°) in the Eastern Himalaya (Baranowski et al. 1984; Drukpa et al. 2006). Chen and Kao (1996) also reported the presence of strike-slip and normal faulting in the Himalayan region. However, strike-slip faulting becomes more frequent near the eastern and western Himalayan syntaxes (Drukpa et al. 2006).

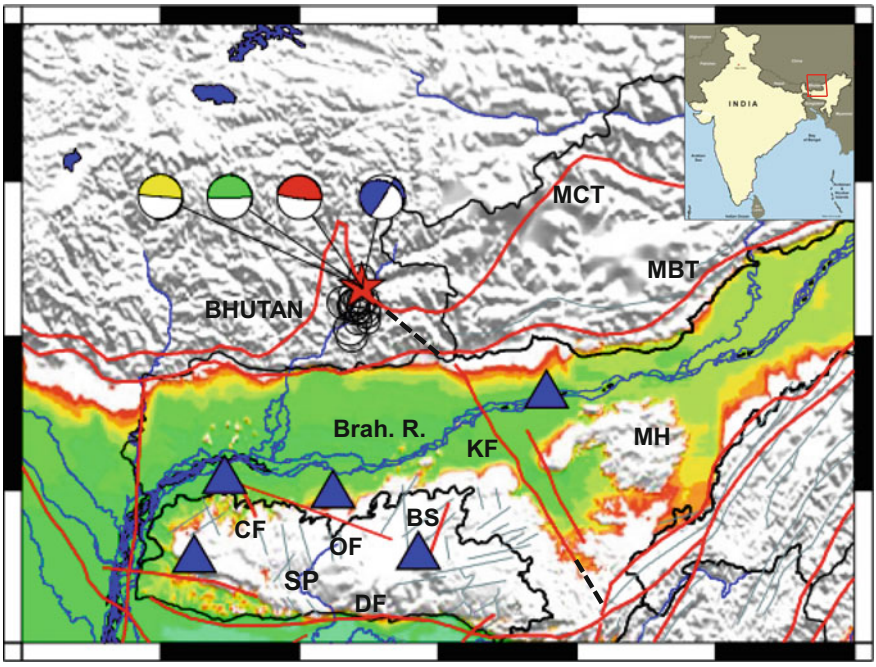

Fig. 1 Tectonic map of Bhutan Himalaya and its adjoining areas (after, GSI 2000) showing main tectonic features of the region. The major tectonic features are MBT: Main Boundary Thrust; MCT: Main Central Thrust; Brah. R.: Brahmaputra River, KF: Kopili fault, MH: Mikir Hills, SP: Shillong plateau; OF: Oldham fault; BS: Barapani Shear zone; DF: Dauki fault; CF: Chedrang fault. The black dotted lines indicate the extended part of Kopili fault. The 21st September 2009 Bhutan Himalaya main shock and 17 significant aftershocks ($M \geq 4.0$) are shown by red stars and open black circle respectively. The blue line indicates the river system. Five stations namely AGA, BOK, SHL, TZR and TRA are also shown as blue triangles. The yellow beach ball indicates the NEIC solution, green beach ball the USGS solution, red beach ball the GCMT solution and the blue beach ball the CSIR-NEIST solution respectively. *Inset* Map of India

3 Databases Used

In order to find out the hypocentral parameters of the 2009 Bhutan earthquake and its aftershocks, digital seismic waveforms from different seismic stations operated by CSIR-NEIST-Jorht are obtained (Table 1). Several locations have been reported for the main shock of the 2009 Bhutan earthquake by different national and international agencies (Table 2). The reported source depth was the most uncertain parameter, ranging from 10 to 15 km. We have reanalyzed the hypocentral parameters using the HYPOCENTER programme of Lienert et al. (1986) and a velocity model proposed by Bhattacharya et al. (2005) for the region. The estimated location errors are ± 2.1 km and ± 5.1 km along the horizontal and depth respectively, and the root mean square error 1.3 s. The same programme is used for locating the aftershocks

Table 1 Station parameters of the seismic stations of North East India

No.	Station	Abb.	Lat (°N)	Long (°E)	Elevation (m)	Seismometer used	Digitizer used
1	Agia	AGA	26.066	90.464	75	Trilium 120P	Guralp DCM
2	Boko	BOK	25.969	91.244	50	Trilium 120P	Guralp DCM
3	Shillong	SHL	25.566	91.859	1590	Trilium 240	TAURAS
4	Tezpur	TZR	26.617	92.783	140	CMG 3ESP	REFTEK
5	Tura	TRA	25.546	90.242	305	Trilium 120P	Guralp DCM

Table 2 Hypocentral parameters of 21st September 2009 Bhutan earthquake given by different national and international agencies

No	Source	Date (YYYY/MM/DD)	OT (HH:MM:SS)	Lat (°N)	Lon (°E)	Depth (km)	Mag (Mw)
1	NEIC	2009/09/21	08:53:06	27.33	91.43	14.0	6.1 (Mw)
	USGS		08:53:06	27.31	91.41	15	6.2 (Mw)
	GCMT		08:53:10	27.2	91.63	12.0	6.1 (Mw)
	ISC		08:53:06	27.36	91.45	16.1	6.2 (Mb)
	CSIR-NEIST		08:53:10	27.32	91.45	15.4	6 (Mw)
	IMD		08:53:04	27.30	91.50	8	6.3 (Mw)

of the 2009 Bhutan earthquake. However, towards retrieval and utilization of waveforms, emphasis should be given to higher signal to noise ratio (clear phases and free from noise) and good azimuthal coverage of the recording stations. Out of these waveforms, inversions are carried out for those waveforms which have undergone very low frequency band pass filtering towards generation of synthetic seismogram.

4 Method of Waveform Inversion

The velocity seismograms selected for waveform inversion are prepared by removal of mean, tapering and band pass filtering. The lower and higher cut off values for the band pass filter depends on the background noise level that exists in the signal as the three component seismograms are filtered using 8-pole Butterworth band pass filter (Scherbaum 1994). The seismograms are filtered within the range 1–2, 2–4 Hz that give smooth noise free waveform to be used for inversion. The observed waveforms are corrected for instrument response so as to get the corresponding ground velocity. Using instrument response, the amplitude in counts are converted into cm/sec unit.

The angle of incidence and the back azimuths for each event are calculated from the hypocentral parameters. The back—azimuth is the angle measured between the vector pointing from the station to the source and the vector pointing from station to the north while the incidence angle is defined as the angle measured between the ray vector at the station (from the source to the station) and the vector pointing from the station straight up. Using these two parameters the observed waveforms are rotated to get vertical, radial and transverse components. After this, the vertical, radial and transverse components are windowed to an appropriate length to include the P and S onsets for each component excluding the later part of the S wave i.e., coda wave, because coda waves are considered to be scattered waves with little relationship to the source process (Aki and Chouet 1975).

4.1 Velocity Model

The first step in inversion procedure is to define a proper crustal velocity model. Use of average crustal velocity model in waveform modeling of local events is difficult because of high frequency contents in the seismograms. A local velocity model can generate the recorded characteristics of near earthquake phases, is very much essential for retrieval of source parameter of small events. Hence, a local crustal velocity model is the prime requirement for waveform modeling. The crustal velocity model along with attenuation parameter helps to determine most important parameter i.e., the Green's function: the seismic impulse response of the Earth. Green's functions when convolved with source time function and observed seismograms produce synthetic seismograms.

For successful applications of full waveform inversion, it is critical to generate a sufficiently accurate starting velocity model in order to allow the misfit function to converge to the acceptable limit. In this study, an initial model is applied to waveform inversion considering the requirement of waveform inversion tool [ISOLA-GUI; (https://github.com/esokos/isola)]. In the waveform inversion tool, there is a fixed option for a maximum of 15 layers [ISOLA-GUI]. For each layer the depth of the top layer, the V_p, V_s (velocities of P and S waves) in km/sec., density in gm/cm^3, Q_p, Q_s (attenuation parameters of P and S waves) are given. As a result the tool generates a graph of V_p and V_s versus depth (km). Many researchers have proposed different velocity model for North East, India using variety of seismological and geophysical methods (e.g., Gupta et al. 1984; Mukhopadhayay et al. 1997; Parvez et al. 2003; Kumar et al. 2004; Mitra et al. 2005; Bhattacharya et al. 2005, 2008). The application of suitable velocity model always plays an important role in waveform inversion. Sensitivity of different velocity models to the focal mechanism solutions of 2009 Bhutan earthquake and its aftershocks are tested first. We observed that the models are sensitive mostly in terms of the DC% and correlation value. The mechanisms obtained using the Bhattacharya et al. (2005) model show high DC% and high correlation values among all other proposed velocity model of North East

Table 3 Crustal velocity model derived by Bhattacharya et al. (2005). The corresponding values of density and attenuation parameters of P and S waves (Q_P and Q_S) are also depicted

Depth (km)	Vp (km/s)	Vs (km/s)	ρ (g/cm^3)	Q_P	Q_S
0.0	5.56	3.19	2.56	300	300
10.0	6.10	3.50	2.94	300	300
20.0	6.45	3.70	3.00	400	200
30.0	6.90	3.96	3.00	400	200
40.0	7.60	4.36	3.30	2000	1000
50.0	8.40	4.82	3.40	2000	1000

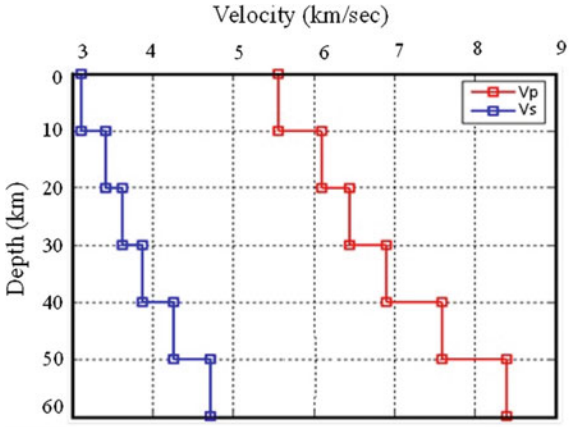

Fig. 2 Velocity model of Bhattacharya et al. (2005) for North East India used in waveform inversion

India region. Hence, in this study also we have selected Bhattacharya et al. (2005) (Table 3; Fig. 2) as the best suitable velocity model of for waveform inversion.

4.2 Steps Involved in Waveform Inversion

The procedure of waveform inversion technique adopted in the present study can be summarized as below. It is assumed that the crustal velocity model used is realistic one and hypocentral parameters of the studied events are accurate. In the process, complete velocity records are used without selecting any particular phases.

(i) The earthquake events recorded by the digital broadband stations are selected on the basis of high signal to noise ratio and clear records of P and S arrival.
(ii) The 3-component digital records are first converted into displacement waveforms.
(iii) The displacement waveforms are then low pass filtered below the corner frequency in order to remove the any offset. The high frequency components

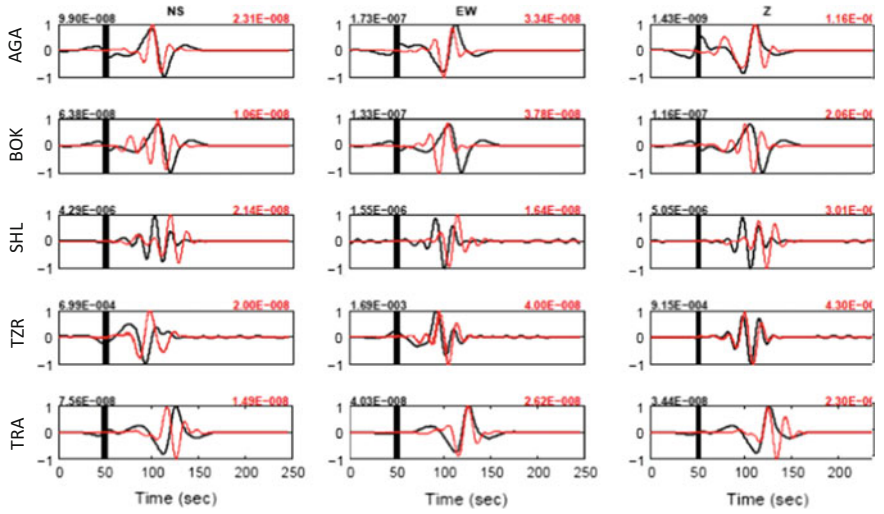

Fig. 3 Waveform inversion for the 2009 Bhutan event; a comparison of synthetic (red lines) and observed (black lines) waveforms at stations AGA, BOK, SHL, TZR and TRA for the preferred focal mechanism solution. X-axis indicates time scale in sec and Y-axis represents amplitude scale in meter. Maximum amplitudes are shown at traces

are excluded because it is difficult to model high frequency components as it requires a precise knowledge of detailed sub-surface crustal velocity model.

(iv) Subsequently resampling of records from a frequency of 100–33 Hz is carried out having with transfer function of the seismometers. Necessary DC removal and Trend line removal is performed.

(v) Green's functions are then computed in the complex spectral domain using the suitable crustal velocity model pertinent to the region at a point source by Discrete Wavenumber (DW) method (Bouchan 1981) and using the program called AXITRA by Coutant (1989). The Green's functions are then convolved with appropriate instrument response and source time function. While calculating the Green's functions, the position of the epicenters are kept fixed.

As we know that the depths of the foci are the most uncertain parameter among all the hypocentral parameters, the depth is allowed to vary in the inversion program from the optimum depth found in the location procedure by up to say ± 5 km in step of 0.5–2 km. Similarly the origin (centroid) time the earthquake was also allowed to vary up to say $\pm(1–2)$ s from that found by location procedure. The time step in the grid search was identical with the sampling interval of 0.01 s (e.g., Fojtikova et al. 2010). The inversion was performed in a frequency band of 0.03–0.05 Hz varying for each event at each depths and times. The final validation of the best fitting solutions was accomplished by comparing the observed and synthetic amplitude waveform.

Table 4 Focal mechanism solutions of 21st September 2009 Bhutan earthquake and its 17 numbers of aftershocks determined through waveform inversion using the broadband data of CSIR-NEIST, Jorhat

No	Source	Date (YYYY/MM/DD)	OT (HH:MM:SS)	Lat (°N)	Long (°E)	Depth (km)	Mag (Mw)	First plane			Second plane			P axis		T axis	
								Strike (°)	Dip (°)	Rake (°)	Strike (°)	Dip (°)	Rake (°)	Azm (°)	Plunge (°)	Azm (°)	Plunge (°)
Main shock parameters																	
1	NEIC	2009/09/21	08:53:06	27.33	91.43	14	6.1 (Mw)	12	4	−173							
	USGS		08:53:06	27.31	91.41	15	6.2 (Mw)	89	86	88							
	GCMT		08:53:10	27.2	91.63	12	6.1 (Mw)	97	84	90							
	ISC		08:53:06	27.36	91.45	16.1	6.2 (Mb)										
	CSIR-NEIST		08:53:10	27.32	91.45	15.4	6 (Mw)	32	86	58	296	31	173	148	35	273	41

(continued)

Table 4 (continued)

No	Source	Date (YYYY/MM/DD)	OT (HH:MM:SS)	Lat (°N)	Long (°E)	Depth (km)	Mag (Mw)	First plane			Second plane			P axis		T axis	
								Strike (°)	Dip (°)	Rake (°)	Strike (°)	Dip (°)	Rake (°)	Azm (°)	Plunge (°)	Azm (°)	Plunge (°)
After shock parameters																	
1	IDC	2009/09/21	09:31:57	27.3	91.45	10											
	ISC		09:31:58	27.34	91.48	15											
	CSIR-NEIST		09:32:01	27	91.38	16.32	3.42	251	77	−161	157	71	−13	115	23	23	4
2	CSIR-NEIST	2009/09/21	09:41:15	27.05	91.37	16.09	3.44	198	85	130	293	40	6	256	30	142	37
3	CSIR-NEIST	2009/09/21	11:07:54	27.2	91.39	14.18	3.4	293	71	4	201	85	161	248	10	156	16
4	CSIR-NEIST	2009/09/21	11:11:37	27.19	91.41	13.72	3.62	180	79	133	281	44	15	238	23	129	40
5	CSIR-NEIST	2009/09/21	11:51:00	27.38	91.45	7.78	3.07	157	84	178	247	88	5	22	3	112	5
6	CSIR-NEIST	2009/09/21	12:31:19	27.1	91.42	16.04	3.15	2	82	−172	272	82	−7	227	11	317	1
7	CSIR-NEIST	2009/09/21	12:37:38	27.15	91.48	8.7	3.29	182	54	31	306	51	47	245	2	152	58
8	IDC	2009/09/21	02:34:02	27.24	91.51	10											

(continued)

Table 4 (continued)

No	Source	Date (YYYY/MM/DD)	OT (HH:MM:SS)	Lat (°N)	Long (°E)	Depth (km)	Mag (Mw)	First plane			Second plane			P axis		T axis	
								Strike (°)	Dip (°)	Rake (°)	Strike (°)	Dip (°)	Rake (°)	Azm (°)	Plunge (°)	Azm (°)	Plunge (°)
	ISC		02:34:09	27.49	91.44	44.4											
	CSIR-NEIST		02:34:07	27.23	91.41	14.64	3.01	234	45	141	353	63	51	109	11	214	55
9	CSIR-NEIST	2009/09/21	04:17:54	27.24	91.46	13.29	3.26	81	88	−175	351	85	−1	306	5	216	2
10	CSIR-NEIST	2009/09/21	04:26:01	27.27	91.36	11.79	2.76	252	54	−8	347	82	−144	215	30	114	19
11	CSIR-NEIST	2009/09/21	05:43:16	27.09	91.5	27.49	2.86	43	66	4	311	85	156	359	14	264	20
12	CSIR-NEIST	2009/09/21	07:58:59	27.16	91.42	11.31	3.02	303	82	−171	212	81	−7	168	11	78	1
13	CSIR-NEIST	2009/09/21	09:45:48	27.27	91.44	11.66	3.07	121	84	174	212	84	5	167	1	77	8
14	CSIR-NEIST	2009/09/21	09:55:47	27.22	91.32	11.92	3.44	212	69	−10	306	79	−158	171	23	78	8
15	CSIR-NEIST	2009/09/21	11:19:52	27.22	91.39	14.25	3.24	351	87	38	259	51	176	118	25	222	29
16	CSIR-NEIST	2009/09/21	11:27:57	27.2	91.4	12.18	3.39	271	64	1	180	88	154	238	18	132	19
17	CSIR-NEIST	2009/09/21	08:27:58	27.19	91.47	10.23	3.5	299	86	3	209	86	176	254	1	164	6

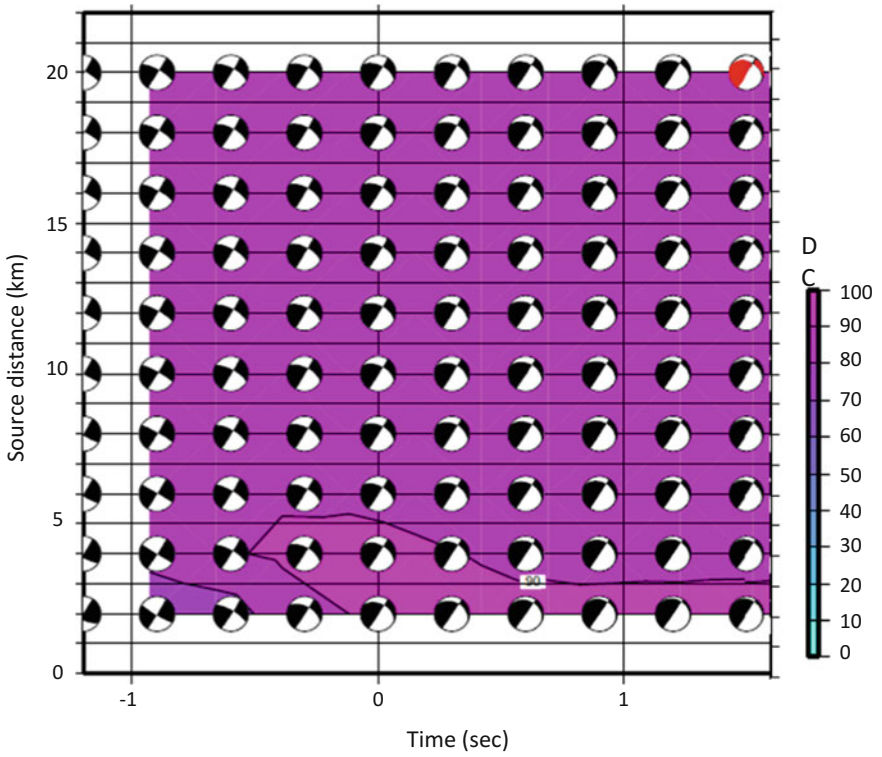

Fig. 4 Plot of source position versus time-shift and focal mechanism for the multiple source inversion. Largest correlation was obtained for source 20 and 1.4 s time shift. Preferred solution is depicted by a red-beachball. Scales for DC% is shown in the right

The inversion procedure inverts the point source moment tensor using Green's functions computed for 1D velocity model. The 1D velocity model may not be perfect and small time shift is required for maximum correlation between the observed and synthetics (Marzooqi et al. 2008). In the inversion technique, the shift is not known and it becomes a non-linear model parameters which has to be inverted along with the moment tensor and optimal source depth. To account for the horizontal mislocation, the synthetics are shifted relative to the observed by changing the origin time few seconds before/after location origin time during the inversion. In this study, the inversion is carried out for full moment tensor. The preferred solution is obtained by a simple grid search over the focal depth with certain steps and also over the origin time between (1–2) s. before/after the location origin time, since the origin time trades off with focal depth. The solution that has a large percentage of variance and double couple component is selected. To accomplish the above procedure the software package by Sokos and Zahradnik (2008) has been used.

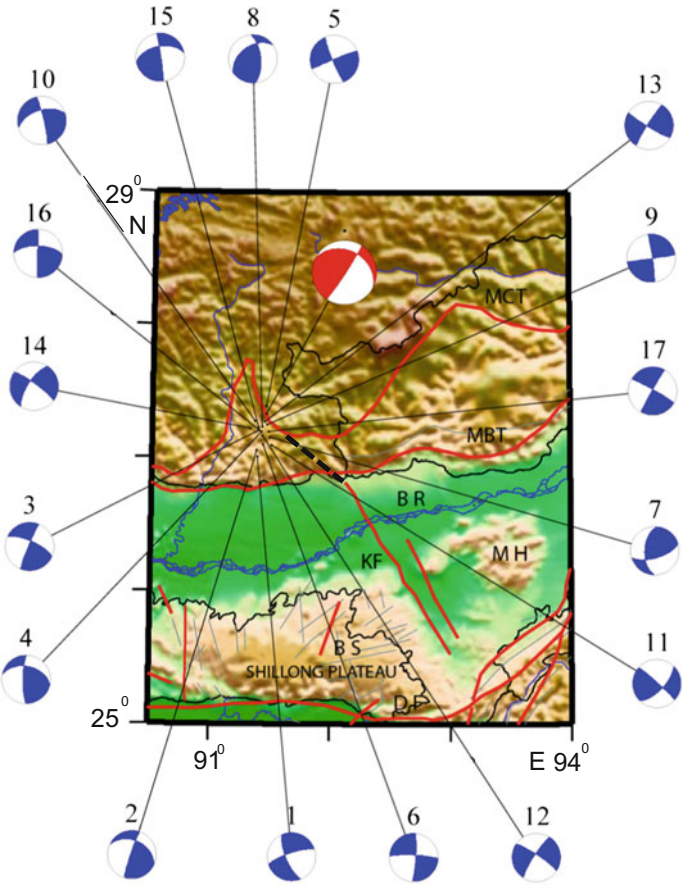

Fig. 5 Focal mechanism solutions of the 2009 Bhutan earthquake (Red beach-ball) and its 17 aftershocks (Blue beach-balls) obtained through waveform inversions. The blue-beach balls are numbered as per Table 4 (Aftershocks Parameters). All other explanations as in Fig. 1

5 Results and Discussions

Focal mechanism solutions of 21st September 2009 Bhutan earthquake along with its 17 aftershocks are determined using waveform inversion technique. There is no doubt that the usage of large station data with good azimuthal coverage yield a reliable focal mechanism solution. But in wave-form inversion technique single station data (less azimuthal coverage) may also become sufficient to get an accurate solution. Several authors made comprehensive studies on the focal mechanism solutions derived from single or double station data e.g. Rao (2009), Delouis and Legrand (1999), Fojtíkova and Zahradnik (2014), Zahradník et al. (2015) etc. In this

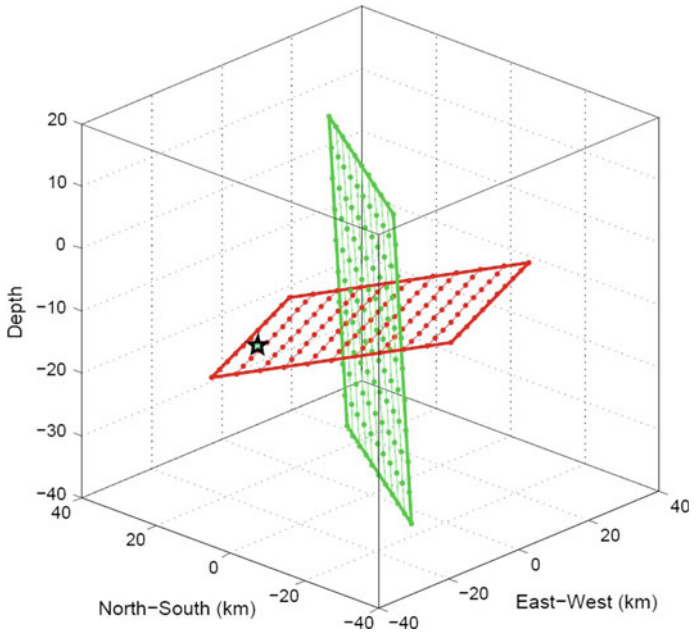

Fig. 6 Fault plane identification of 2009 Bhutan event. Two nodal planes (red and green planes) passing through the centroid. Hypocentre exists on one of the nodal planes (red planes), and thus indicates the fault plane

study, Seismic waveform data from five stations namely AGA, BOK, SHL, TZR and TRA are used in the search of focal mechanism.

The inversion for 2009 Bhutan earthquake (Date: 21-09-2009, OT: 08 h:53 min:10.4 s, Lat. 27.329°, Long. 91.459°, Depth. 15.4 km, $M_D = 3.5$) is performed at a starting depth of 5 km (15.4 km being the actual depth) having a spacing of 2 km with 10 trial source positions. The used frequency band for the inversion is fixed at (0.03–0.05 Hz) with cosine tapering applied in order to obtain the detailed information about the source rupture process. The best waveform match between observed and synthetic (Fig. 3) is obtained with the calculation of Green's function at the epicentral distance of 155, 153, 171, 232 and 200 km respectively for stations namely BOK, TZR, AGA, TRA, and SHL. Ultimately a preferred solution is obtained (red beach ball) based on maximum correlation between source position and time-shift. Figure 4 shows that the preferred solution (red beach ball) differs from the nearby solutions in terms of DC percentage and correlation value. The focal parameters are illustrated in Table 4.

As illustrated in Fig. 4, it is ascertained from correlation value that the preferred solution is well correlated at a depth of 20 km for a time-shift of 1.4 s having a DC% of 82. Thus, we can conclude from the observation that the 2009 Bhutan event is characterized by thrust with strike-slip faulting; all of the 17 aftershocks are also consistent with the main event (Fig. 5).

Earthquake source parameters were used to identify the orientation of event's fault plane. To identify the true fault plane orientation, the H (Hypocentre)—C (Centroid) method was used with combined knowledge of the centroid position, MT solution (nodal planes), and hypocenter key to identify this fault plane. The nodal planes pass through C, with the fault plane corresponding to the plane that also passes through H. If the hypocentre, centroid and nodal planes are consistent, they enable the identification of which nodal plane is the fault plane (Zahradnik et al. 2008).

The hypocenter coordinate for Bhutan event is obtained using CSIR-NEIST data whereas centroid coordinate is obtained using GCMT data. Based on the analysis results, the Bhutan event has hypocentre-centroid distance of 22.42 km. The fault plane 1 (green plane) is characterized by strike = 32°; dip = 86°; rake = 58° with distance of 22.27 km from the hypocentre. The fault plane 2 (red plane) is characterized by strike = 296°; dip = 31° and rake = 173° with a distance of 2.05 km from the hypocentre. The distance of fault plane 2 to the hypocentre is closer than fault plane 1. Therefore, the real fault plane is fault plane 2 as shown in Fig. 6.

6 Conclusion

The Mw 6.1 2009 Bhutan earthquake is used for the study of seismotectonics of the Bhutan Himalaya through a state of art technique called waveform inversion of seismic waves. Focal mechanism solutions of 2009 Bhutan earthquake is found to be thrust with strike slip faulting which clearly indicates the existence of transverse faults in the region. The same observation was also reported by Kayal et al. (2010). The geologically mapped curvilinear structure of the Main Central Thrust (MCT) in the Himalaya, where the epicentre of the Bhutan earthquake is located, is possibly caused by the transverse Kopili fault beneath the MCT. Further, identification of the true fault plane orientation is made by using H-C method. The distance of fault plane 2 (strike = 296°; dip = 31° and rake = 173°) to the hypocentre is closer than the fault plane 1 (strike = 32°; dip = 86°; rake = 58°). Therefore, the real fault plane is fault plane 2. The plane 2 coincides with the orientation of the extended Kopili fault in the Bhutan Himalaya region. The P-axis orientations of the 2009 Bhutan earthquake and most of its aftershocks are found to be nearly along N-S direction which display the northward underthrusting of the Indian plate to the Eurasian plate along Bhutan Himalaya.

Acknowledgements We thank Dr. D. Ramaiah FNASc, FNA, Director, CSIR-North East Institute of Science and Technology (CSIR-NEIST), Jorhat, for his kind support and encouragement in carrying out this work. We thank Prof. Harsh K. Gupta, Chairman, Research Council, CSIR-NEIST-J for his encouragement. We also thank Prof. J. R. Kayal, Visiting Professor, ISR, Gujarat, India and Dr. Saurabh Baruah, Head, GSTD, CSIR-NEIST-Jorhat, Assam, India for their help. Dr. Sebastiano D'Amico, Editor and the reviewers are thankfully acknowledged for their constructive comments. The Science and Engineering Research Board (SERB), Government of India provided the financial support for this under Young Scientist Scheme, vide Sanction No. SR/FTP/ES-121/2014.

References

Aki K, Chouet B (1975) Origin of coda waves: source, attenuation, and scattering effects. J Geophys Res (Solid Earth and Planets) 80:3322–3342. https://doi.org/10.1029/jb080i023p03322

Baranowski J, Armbruster J, Seeber L, Molner P (1984) Focal depths and fault plane solutions of earthquakes and active tectonics of the Himalaya. J Geophys Res 89(B8):6918–6928

Bhattacharya PM, Pujol J, Mazumdar RK, Kayal JR (2005) Relocation of earthquakes in the Northeast India region using joint Hypocenter determination method. Curr Sci 89(8):1404–1413

Bhattacharya PM, Mukhopadhyay S, Mazumdar RK, Kayal JR (2008) 3-D seismic structure of the northeast India region and its implications for local and regional tectonics. J Asian Earth Sci 33:25–41

Bouchon M (1981) A simple method to calculate Green's functions for elastic layered media. Bull Seism Soc Am 71:959–971

Chen WP, Kao H (1996) Seismotectonics of Asia: some recent progress. In: Yin A, Harrison M (eds) The tectonic evolution of Asia. Cambridge University Press, Cambridge, pp 37–62

Coutant O (1989) Program of numerical simulation AXITRA, Research Report LGIT, Grenoble in French

Curray JR, Emmel FJ, Moore DG, Raitt RW (1982) Structure tectonics and geological history of the northeastern Indian Ocean. In: Nairn AEM, Stehli FG (eds) The ocean basins and margins, The India Ocean, vol VI. Plenum, New York, pp 399–450

Delouis B, Legrand D (1999) Focal mechanism determination and identification of the fault plane of earthquakes using only one or two near-source seismic recordings. Seismol Soc Am Bull 89:1558–1574

Drukpa D, Velasco AA, Doser DI (2006) Seismicity in the Kingdom of Bhutan (1937–2003): evidence for crustal transcurrent deformation. J Geophys Res 111:B06301. https://doi.org/10.1029/2004jb003087

Fitch TJ (1970) Earthquake mechanisms in the Himalaya, Burmese and Andaman Regions and continental tectonics in Central Asia. J Geophys Res 75:2699–2709

Fojtikova L, Vavrycuk V, Cipciar A, Madaras J (2010) Focal mechanisms of micro-earthquakes in the Dobra Voda seismoactive area in the Male Karpaty Mts. (Little Carpathians), Slovakia. Tectonophysics 492:213–229. https://doi.org/10.1016/j.tecto.2010.06.007

Fojtíkova L, Zahradnik J (2014) A new strategy for weak events in sparse networks: the first-motion polarity solutions constrained by single-station wave-form inversion. Seismol Res Lett 85(6):1265–1274. http://dx.doi.org/10.1785/0220140072

Gansser A (1964) Geology of the Himalaya. London (Inter Science), p 289

Gansser A (1993) The Himalayas seen from Bhutan. J Geol B-A Band 136:335–346. ISSN: 0016-7800

Grujic D, Casey M, Davidson C, Hollister LS, Kundig R, Pavlis T, Schmid S (1996) Ductile extrusion of the higher Himalayan crystalline in Bhutan: evidence from quartz microfabrics. Tectonophysics 260:21–43

Grujic D, Hollister L, Parrish R (2002) Himalayan metamorphic sequence as an orogenic channel: insight from Bhutan. Earth Planet Sci Lett 198:177–191

Grujic D, Coutand I, Bookhagen B, Bonnet S, Blythe A, Duncan C (2006) Climatic forcing of erosion, landscape, and tectonics in the Bhutan Himalayas. Geology 34:801–804

GSI (2000) Seismotectonic atlas of India and its environs, geological survey. India Pub. 86 pp

Gupta HK, Singh SC, Dutta TK, Saikia MM (1984) Recent investigations of North East seismicity. In: Gongxu G, Xing-Yuan M (eds) Proceedings of the international symposium continental seismicity and earthquake prediction. Seismological Press. Beijing, pp 63–71

Kayal JR, Arefiev S, Baruah S, Tatevossian R, Gogoi N, Sanoujam M, Gautam JL, Hazarika D, Bora D (2010) The 2009 Bhutan and Assam felt earthquakes (Mw 6.3 and 5.1) at the Kopili fault in the northeast Himalaya region. Geomat Nat Hazards Risk 1:273–281

Kumar MR, Raju PS, Devi EU, Saul J, Ramesh DS (2004) Crustal structure variations in northeast India from converted phases. Geophys Res Lett 31:1–4. https://doi.org/10.1029/2004GL020576

Lienert BR, Berg BE, Frazer LN (1986) Hypocenter: an earthquake location method using centered, scaled and adaptively damped least squares. Bull Seism Soc Am 76:771–783

Marzooqi YAl , Abou Elenean KM, Megahed AS, El-Hussain I, Rodgers A, Al Khatibi E (2008) Source parameters of March 10 and September 13, 2007, united Arab Emiratus earthuqkae. Tectonophysics, 460:237–247

Mckenzie DP, Sclater JG (1971) The evolution of the Indian Ocean since the late cretaceous. Geophys J 24:437–528

Mitchell AHG (1981) Phanerozoic plate boundaries in mainland SE Asia, the Himalayas and Tibet. Geol Soc London J 138:109–122

Mitra S, Pristley K, Bhattacharya A, Gaur VK (2005) Crustal structure and earthquake focal depths beneath northeastern India and southern Tibet. Geophys J Int 160:227–248

Molnar P, Tapponnier P (1975) Cenozoic tectonics of Asia: effects of a continental collision. Science 189:419–425

Mukhopadhyay S, Chander R, Khattri KN (1997) Crustal properties in the epicentral tract of the Great 1897 Assam Earthquake, northeastern India. Tectonophysics 283:311–330

Nandy DR (2001) Geodynamics of Northeastern India and the adjoining region. ACB publications, Calcutta

Ni J, Barazangi M (1984) Seismotectonics of the Himalayan collision zone: geometry of the underthrusting Indian plate beneath the Himalaya. J Geophys Res 89:1147–1163

Parvez IA, Vaccari F, Panza GF (2003) A deterministic seismic hazard map of India and adjacent areas. Geophys J Int 155:489–508

Pradhan R, Prajapati S, Chopra S, Kumar A, Bansal BK, Reddy CD (2013) Causative source of Mw 6.9 Sikkim-Nepal border earthquake of September 2011: GPS baseline observations and strain analysis. J Asian Earth Sci 70–71:179–192

Rao NP (2009) Single station moment tensor inversion for focal mechanisms of Indian intra-plate earthquakes. Curr Sci 77(9):1184–1188

Ravi Kumar M, Hazarika P, Prasad GS, Singh A, Saha S (2012) Tectonic implications of the September 2011 Sikkim earthquake and its aftershocks. Curr Sci 102:788–792

Scherbaum F (1994) Modelling the Roermond earthquake of 1992 April 13 by stochastic simulation of its high-frequency strong ground motion. Geophys J Inr 119:31–43

Seeber L, Armbruster JG (1981) Great detachment earthquakes along the Himalayan arc and long-term forecasting. In: Earthquake prediction—An international review. Manrice Ewing Serires, American Geophysical Union, vol 4, pp 259–277

Searle MP (1996) Cooling history, erosion, exhumation, and kinematics of the Himalayan-Karakoram-Tibet orogenic belt. In: Yin A, Harrison M (eds) The tectonic evolution of Asia. Cambridge University Press, New York, pp 110–137

Sokos E, Zahradnik J (2008) ISOLA—A Fortran code and Matlab GUI to perform multiple-point source inversion of seismic data. Comput Geosci 34:967–977

Zahradnik J, Gallovic F, Sokos E, Serpetsidaki A, Tselentis G-A (2008) Quick fault-plane identification by a geometrical method: application to the Mw 6.2 Leonidio earthquake, 6 January 2008, Greece. Seismol Res Lett 79(5):653–662

Zahradník J, Fojtíkova L, Carvalho J, Barros LV, Sokos E, Janský J (2015) Compromising polarity and waveform constraints in focal-mechanism solutions; the Mara Rosa 2010 Mw 4 central Brazil earthquake revisited. J Sci Am Earth Sci 63:323–333. https://doi.org/10.1016/j.jsames.2015.08.011

Zhao W, Nelson KD, Project INDEPTH Team (1993) Deep seismic reflection evidence for continental underthrusting beneath southern Tibet. Nature 366:557–559